

# The study of high-dc electric field effect on the conduction of $V_2O_5$ –Sb– $TeO_2$ glasses and the applicability of an electrothermal model

Dariush Souri · Raziye Ghasemi · Mahdiyeh Shiravand

Received: 2 July 2014 / Accepted: 24 December 2014 / Published online: 22 January 2015  
© Springer Science+Business Media New York 2015

**Abstract** Ternary  $(60-x)V_2O_5-xSb-40TeO_2$  oxide glasses (with  $0 \leq x \leq 15$  in mol%), prepared using the usual melt quenching method, were investigated electrically (at the presence of high-dc electric fields) within the temperature range of 298–375.3 K at different electrode distances. The current–voltage characteristics show increasing deviations from Ohm’s law at electric fields of about  $>10^3$  V/cm. This behavior can be attributed to the Pool–Frenkel effect, which usually occurs at the mentioned electric fields. At higher fields, switching (from low conduction state to higher conduction state) or negative resistance phenomena were observed at a threshold voltage ( $V_{th}$ ). The threshold voltage for beginning the switching/negative resistance shows a decreasing trend with increasing in temperature and also with decreasing of electrode distance. An electrothermal model (based on the Joule heating effect in the current filament) is proposed to interpret the observed electrical properties. Also, the lowering factor of potential barrier ( $\beta_{PF}$ ) in Pool–Frenkel effect, heat dissipation factor, and electrical activation energy of the present samples were determined. In each sample, the increase of  $\beta_{PF}$  with temperature can explain the phonon-assisted hopping conduction.

## Introduction

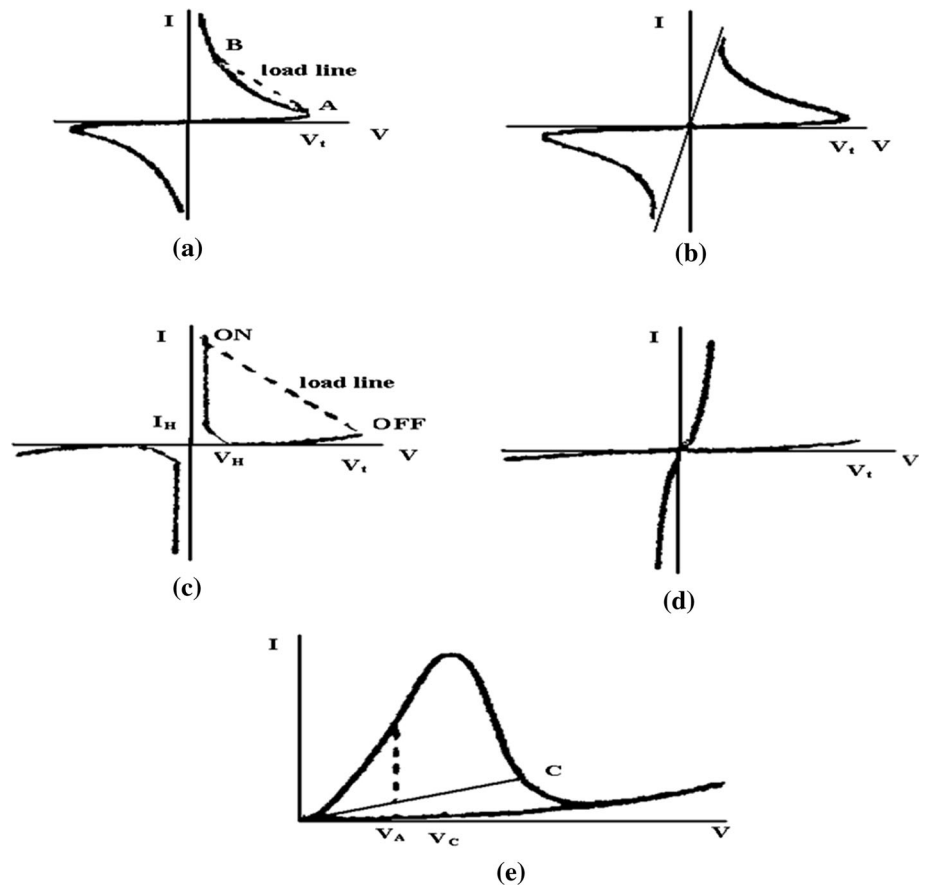
Amorphous materials that show negative resistance or switching behavior first have been reported by many authors [1–8]. Semiconducting glasses and specially

oxide glasses containing transition metal oxides (TMOs) can exhibit an OFF–ON transition from high to low resistive state (switching) at a certain voltage. The dc voltage, at which the transition from OFF to ON state takes place, is called the “threshold voltage” and termed as  $V_{th}$  [2–10].  $V_{th}$  depends on different parameters such as temperature, electrode distance, and composition of the samples. Oxide glasses have attracted a great interest fundamentally and technologically owing to their potential applications as cathodes for lithium batteries [11, 12], electronic and optoelectronic devices [13–15], and high-speed and high-capacity nonvolatile memories such as flash memories [16]; therefore, the investigation of the I–V characteristics and switching behavior of such amorphous semiconductors can play an important role to understand the mechanism of negative resistance/switching and also to find a suitable material for device applications such as fast electrical switches. At high electric fields, most of oxide glasses such as  $TeO_2$ – $V_2O_5$ – $MoO_3$  [7, 9, 10],  $P_2O_5$ – $Li_2MoO_4$ – $Li_2O$  and  $P_2O_5$ – $Na_2MoO_4$ – $Na_2O$  [5] show non-ohmic conduction leading to negative resistance/switching phenomenon. Such nonlinear current–voltage (I–V) characteristics have been explained up on the Pool–Frenkel effect. Two kinds of switching phenomena (i.e., memory and threshold) must be distinguished [1, 2, 7, 8]. The most frequent anomalous conduction types observed in semiconducting oxide glasses are summarized in Fig. 1 [17–22]. The switching effect has given rise to many models, which the most frequent are thermal model [18, 23], electrothermal model [18], and electronic model [18, 24].

In the thermal mechanism, the transition between insulating to a conducting state is caused mainly by a joule heating effect, which is responsible for increasing of the temperature with subsequent reversible phase

D. Souri (✉) · R. Ghasemi · M. Shiravand  
Department of Physics, Faculty of Science, Malayer University,  
Malayer, Iran  
e-mail: d.souri@gmail.com; d.souri@malayeru.ac.ir

**Fig. 1** Different types of negative resistance/switching behavior [19], **a** negative resistance without memory **b** negative resistance with memory **c** threshold switching **d** memory switching **e** voltage-controlled negative resistance



transition. The electronic mechanism, developed for switching in thin films, assumes no heating of samples and results from space charges localized at the electrodes. Electrothermal mechanism, as a hybrid of two other mechanisms, is associated with formation of both hot conductive channels in the material and space charges at electrodes [19].

In our previous works, we have studied the optical and some thermal properties [15] and also the low-field dc conductivity [17] of the present glasses; thus, because of (i) fundamentally and technologically mentioned importance of tellurate-vanadate oxide glasses and (ii) lack of any report on the high-field conduction of these glasses, this work aims to (a) study the negative resistance or switching phenomena for  $V_2O_5-Sb-TeO_2$  glasses to elucidate the effect of different factors such as temperature and electrode distance and also to complete the electrical data reported in [17], (b) study the high-field electrical behavior (Pool-Frenkel effect), (c) verify and certify the electrothermal mechanism of negative resistance phenomena and obtaining the electrical activation energy and heat dissipation factor, and (d) report and explain the compositional dependence of threshold voltage and also lowering factor  $\beta_{PF}$ .

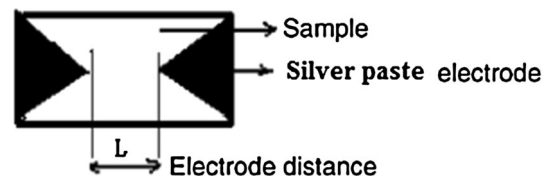


**Fig. 2** Electrode configuration (gap-type)

**Experimental procedure**

For the present samples, details of sample preparation and structural and thermal characterization using XRD, SEM, and DSC have been presented in our recent works [15, 17]. Ternary  $(60-x)V_2O_5-xSb-40TeO_2$  glasses, hereafter, are termed as TVSbx. Carefully surface-polished bulk samples were used for electrical measurements; electrical measurements were done with gap-type electrode configuration (see Fig. 2), using a high-voltage power supply (Molian Toos, 0–5 kV, Iran) and sensitive multimeters (TTi, 196, High-resolution computing multimeter, England).

For each sample, the I–V characteristic was measured to verify the ohmic properties of the contacts; in other word, ohmic behavior was ascertained from the linearity of I–V curves at low electric field.

## Results

### Structural features

As reported in our recent works [15, 17], XRD patterns of TVSbx samples confirm their amorphous feature, except for TVSb12 and 15. Up on these reports, XRD pattern of TVSb12 shows some crystalline peaks at  $2\theta \approx 49.78^\circ$  and  $49.66^\circ$  (matched with  $\text{VO}_2$  crystal phase) and also at  $2\theta \approx 27.44^\circ$  and  $35.2^\circ$ , which were matched with the vanadium–antimony (SbVO) phase. Besides, the microcrystalline phases have been certified by SEM images [17]. Also, glassy nature, thermal stability, and glass forming tendency of these samples have been reported in our recent work [15].

### Electrical behavior

Figures 3 and 4 show the typical I–V curves for TVSb5 at different temperatures and for TVSb10 at different electrode distances. From Fig. 3, one can observe the increase

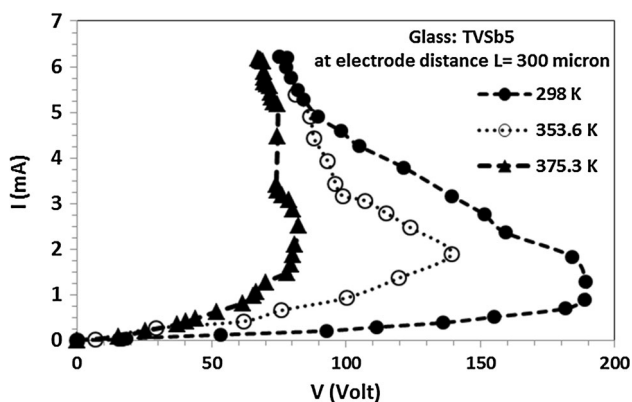


**Fig. 3** Current–voltage characteristics of TVSb5 at different temperatures at a fixed electrode distance

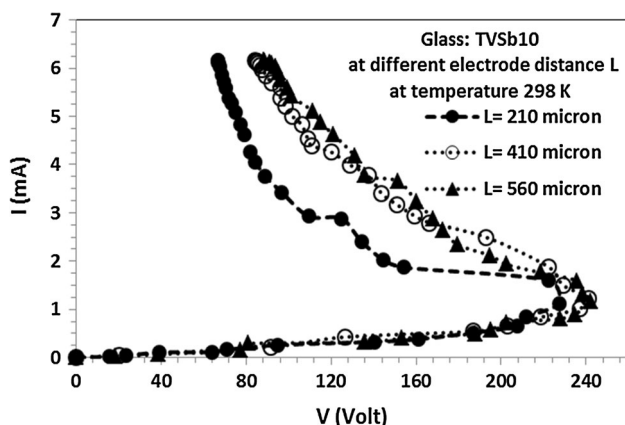


**Fig. 4** Current–voltage characteristics of TVSb10 at different electrodes distances at a fixed temperature

of electrical conduction of all glasses with increasing the temperature, which reveals the semiconducting nature of these samples. Also, during the experiments, influence of Sb content on the I–V characteristics was evident. The obtained results show the increasing of resistivity with increasing of Sb content; this result is in agreement with the results of low-field dc conductivities reported in ref.17. It can be observed that after the ohmic region (linear I–V region), the current–voltage characteristics show increasing deviations from Ohm’s law at electric fields of about  $>10^3$  V/cm; as discussed later, this behavior can be attributed to Pool–Frenkel effect, which usually occurs at the above-mentioned electric fields. At higher fields, switching (from high to low resistive state) or negative resistance phenomena were observed at a threshold voltage ( $V_{th}$ ). As is evident from Figs. 3 and 4, the threshold voltage for the onset of switching/negative resistance shows a decreasing trend with increasing in temperature and with decreasing of electrode distance. All  $V_{th}$  data, obtained at different temperatures and electrode distances, are presented in Tables 1 and 2. The mentioned electrical behavior is interpreted by an electrothermal model based on the Joule heating effect in the current filament, which proposes the probable formation of crystalline phase in the current filament of amorphous matrix. Details of proposed model and further discussions are presented in “[Structural characteristics](#)” section

## Discussion

### Structural characteristics

As have been presented [15, 17] and in [Structural features](#) section, the structural changes in samples with  $x \geq 12$  had distinguished effects on electrical and optical properties [15, 17], and it should be mentioned that may affect on high-field conduction and threshold voltage. It has been reported that the mentioned structural changes and existence of microcrystalline phases in TVSb12 and 15 cause the decreasing trend in electrical activation energy at low electric field experiments [17]. These effects are presented and discussed in continue (see “[High electric field properties and electrothermal mechanism for negative resistance behaviour](#)” section).

### High electric field properties and electrothermal mechanism for negative resistance behavior

The temperature dependence of the I–V characteristics is an important factor to define a negative resistance (NR)/switching material for technological applications. In this study, the effect of the temperature on the negative

**Table 1** The data of threshold voltage ( $V_{th}$ ) and lowering factor of potential barrier ( $\beta_{PF}$ ) at different temperatures, for TVSbx glasses

Glass name	Composition	Electrode distance (micron)	Temperature (K)	$V_{th}$ (Volt)	$\beta_{PF}$ (Vm) <sup>1/2</sup>
TVSb0	60V <sub>2</sub> O <sub>5</sub> – 40TeO <sub>2</sub>	160	298	287.15	9.99
			353.66	139.21	15.856
			375.33	82.22	28.180
TVSb5	55V <sub>2</sub> O <sub>5</sub> – 40TeO <sub>2</sub> – 5Sb	300	298	189.07	13.27
			353.66	139.21	15.856
			375.33	82.22	28.180
TVSb8	52V <sub>2</sub> O <sub>5</sub> – 40TeO <sub>2</sub> – 8Sb	240	298	251.45	6.2
			345	105.46	15.684
			366	75.51	25.422
TVSb10	50V <sub>2</sub> O <sub>5</sub> – 40TeO <sub>2</sub> – 10Sb	210	298	227.38	8.014
			348	140.75	12.151
			370.66	74.72	20.768
TVSb12	48V <sub>2</sub> O <sub>5</sub> – 40TeO <sub>2</sub> – 12Sb	240	298	207.62	11.375
			339.33	141.51	11.806
			369	91.57	25.163
TVSb15	45V <sub>2</sub> O <sub>5</sub> – 40TeO <sub>2</sub> – 15Sb	340	298	183.03	9.393
			340	102.04	20.941
			370.33	81.69	21.199

For each sample, at a constant electrode distance, the decreasing of  $V_{th}$  with increasing of temperature is evident. Because of the semiconducting nature of these samples, increasing of temperature causes to increasing of dc conductivity and also decreasing the  $V_{th}$

**Table 2** Threshold voltage ( $V_{th}$ ) at different electrode distances for TVSbx glasses (at room temperature 298 K)

Glass name	Electrode distance (micron)	$V_{th}$
TVSb0	160	287.15
	260	318.3
TVSb5	300	189.07
	380	222.33
TVSb8	150	217.34
	210	241.04
	240	251.45
TVSb10	210	227.38
	410	241.45
	560	242.05
TVSb12	240	207.62
	390	210.34
	540	220.22
TVSb15	340	183.03
	390	197.23
	410	205.78

For each sample, at a constant temperature, the increasing of  $V_{th}$  with increasing the electrode distance is evident. Increasing in electrode distance causes to increasing of the resistivity of the material between the electrodes and also increasing the  $V_{th}$

resistance/switching behavior has been investigated. Table 1 presents the temperature dependence of the threshold voltage for the present samples. The obtained results reveal that all studied glasses show similar behavior, which can be attributed to the thermal effects during NR/switching.

Also, during the experiments, it was noted that at same condition of temperature and electrode distance,  $V_{th}$  increased with increasing of Sb content for  $0 \leq x \leq 10$  and so decreases for TVSb12 and 15. The differential scanning calorimetry (DSC) could be used to specify the variation of  $V_{th}$  with composition. In all semiconductors, conditions may occur in which the self-generated Joule heat exceeds the capacity of the system to dissipate it. The current increases with temperature, which leads to more Joule self-heating and the consequent thermal runaway. Oxide glassy semiconductors have large negative temperature coefficients of electrical resistivity and low thermal conductivities, so thermal runaway must always be considered as a possible breakdown mechanism in high electric fields. Even if it is not the dominant mechanism which gives rise to the switching process, thermal effects are likely to be present even in thin films and their influence must be understood [7, 19, 23]. It is important to note that no one of the NR/switching models can explain the NR/switching phenomena and the effects of a high electric field on the glasses. If the internal temperature of the samples in the current filament exceeds to glass transition temperature  $T_g$ , the structural change (crystallization filament in the glassy matrix) is possible. Therefore, the compositional dependence of  $V_{th}$  is explainable using the  $T_g$  data. The DSC data of these glasses [15] show the increasing of  $T_g$  with increasing in Sb content and then more rigidity of the sample. These data imply to that the structural change is less possible with increasing of Sb content. On the other hand,  $T_g$  data are not sufficient to explain the  $V_{th}$  variations; in other word, nevertheless of regular increasing of  $T_g$  with Sb content,  $V_{th}$  has an

increasing trend up to  $x = 10$  mol% and then decreasing trend for  $x > 10$  mol%. Thus, it needs to be clarified using an additive parameter; as reported recently [15], another useful parameter is glass thermal stability ( $S = T_{Cr} - T_g$ ;  $T_{Cr}$  is the crystallization temperature), which defines the stability of glass against thermal shocks and against structural changes. The present glasses have increasing trend in  $S$  up to TVSb12, although TVSb12 and 15 have good stability [15]. This result can justify the two variation regions of  $V_{th}$ . Also, as can be observed in “Structural characteristics” section, it has been reported that the mentioned structural changes, existence of microcrystalline phases in TVSb12 and 15, and the decreasing trend in glass stability for TVSb12 and 15 cause the decreasing trend in electrical activation energy at low electric field experiments [17]; this result can justify the decrease of  $V_{th}$  for  $x \geq 12$  mol%. These results can be justified from the data of glass forming tendency ( $K_{gl}$ ). For the present glasses, the data of  $K_{gl}$  have been reported in our recent work [15]; results show an increasing trend of  $K_{gl}$  for  $0 \leq x \leq 12$  and then a decreasing trend for  $12 \leq x \leq 15$  [15]; therefore, these reports justify the variation of  $V_{th}$ .

Besides temperature, another important factor affecting on the threshold voltage must be the electrode distance ( $L$ ) [7, 19]. The present study reveals that  $V_{th}$  increases with increasing electrode distances for all samples, see Table 2. Although, one cannot specify the real dominant mechanism of NR/switching, but it seems to be more electronic for the electrode distances less than few microns in thin films, and therefore electrothermal for bulk samples. Generally, as presented in the following, we can conclude that NR/switching process in these glasses is on the basis of the electrothermal mechanism.

Generally, the electrical conductivity of non-adiabatic small polaron hopping (NASPH) is thermally activated in the high temperature range and is known by the relation [12, 17]:

$$\sigma = (\sigma_{\infty}/T) \exp\left[-\frac{E_a}{kT}\right], \quad (1)$$

where  $k$  is the Boltzmann constant,  $\sigma_{\infty}$  is the pre-exponential factor (the conductivity at infinite temperature), and  $E_a$  is the activation energy. To justify the electrothermal mechanism, we can legally assume that the I–V characteristic is principally described by an ohmic dependence  $V = R(T)I$ , with  $T$  the real temperature of the sample. This temperature dependence on injected electrical power according to the following relation proposed to be

$$T = T_0 + \alpha VI, \quad (2)$$

where  $\alpha$  is the heat dissipation factor resulting from thermal conductivity and  $T_0$  is the sample temperature for zero current. Using Eqs. 1 and 2, we have

$$VI = \frac{E_a}{\alpha k \ln(V/R_{\infty}I)} - \frac{T_0}{\alpha}, \quad (3)$$

where  $R_{\infty}$  is the electrical resistance of sample at infinite temperature.  $R_{\infty}$  values have been deduced from ref. 17. From Eq. 3, it is clear that  $E_a$  (hereafter termed as  $E_a^{IV}$  to be distinguished from electrical activation energy obtained from conductivity measurements at low fields  $E_a^{cond}$  [17]) and  $\alpha$  can be determined from the slope and intercept of the linear part of  $VI$  versus  $1/\ln(V/R_{\infty}I)$  plots. In this work,  $E_a^{IV}$  and  $\alpha$  were determined from the slope and intercept of the linear part of  $VI$  versus  $1/\ln(V/R_{\infty}I)$  plots. As can be followed from our previous work [17], it should be mentioned that  $E_a^{cond}$  has been obtained from the slope of  $\ln\sigma$ – $T^{-1}$  curves at low electric fields. Using Figs. 3 and 4, typical experimental plots of  $VI$  versus  $1/\ln(V/R_{\infty}I)$  are shown in Figs. 5 and 6. Obtained values of  $E_a^{IV}$  and  $\alpha$  are listed in Table 3. The values of  $E_a^{IV}$  are in the same order of  $E_a^{cond}$  values reported in [17]. For the present samples, these low values of  $E_a$  obtained from low to high field experiments

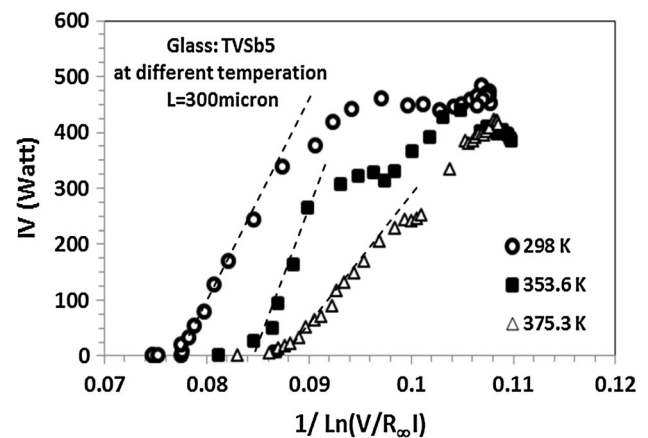


**Fig. 5** Plots of the electrical power vs.  $1/\ln(V/R_{\infty}I)$  for TVSb5 at different temperatures. (Dashed lines show the linear parts, which are used to obtain  $E_a^{IV}$  and  $\alpha$ , and are drawn as a guide for the eye)

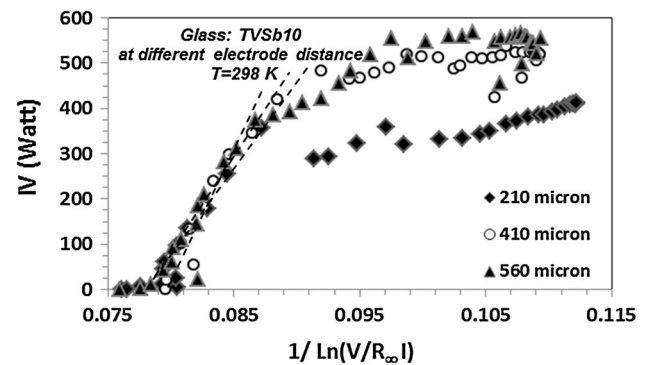


**Fig. 6** Plots of the electrical power vs.  $1/\ln(V/R_{\infty}I)$  for TVSb10 at different electrode distances. (Dashed lines show the linear parts, which are used to obtain  $E_a^{IV}$  and  $\alpha$ , and are drawn as a guide for the eye)



**Table 3** Values of zero-field temperature ( $T_0$ ), heat dissipation factor ( $\alpha$ ) obtained from the intercept of the linear part of  $VI-1/\ln(V/R_\infty I)$  plots, activation energy ( $E_a$ ) obtained from the slope of the linear part of  $VI-1/\ln(V/R_\infty I)$  plots, and sample resistance at infinite temperature ( $R_\infty$ ), for TVSbx glasses

Glass	$T_0$ (K)	$\alpha$ (K W <sup>-1</sup> )	$E_a^{IV}$ (eV)	$E_a^{cond}$ (eV) [17]	$R_\infty$ ( $\Omega$ ) [17]
TVSb5	298	0.1170	0.333	0.338	0.0011
	353.6	0.0865	0.358		
	375	0.2254	0.372		
TVSb8	298	0.4428	0.396	0.375	0.0010
	345	0.1796	0.361		
	366	0.1627	0.354		
TVSb10	298	0.0982	0.329	0.389	0.0015
	348	0.0963	0.352		
	370.6	0.0994	0.327		
TVSb12	298	0.1755	0.335	0.401	0.0015
	339.3	0.1239	0.346		
	369	0.1649	0.350		
TVSb15	298	0.1469	0.326	0.411	0.0015
	340	0.1388	0.331		
	370.3	0.0942	0.334		

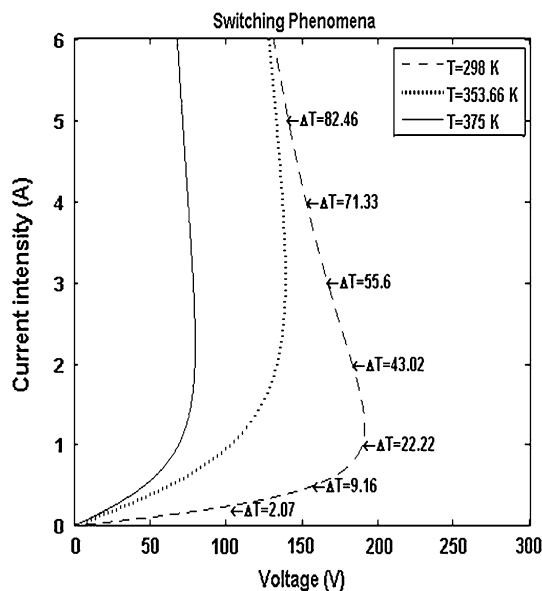


**Fig. 7** Computer-simulated I–V plots at different  $T_0$  values.  $\Delta T = T - T_0$  shows temperature increase in the bulk of the samples and is shown typically for TVSb5)

justify the hopping conduction of carriers, not band to band electrical transition (which also can be realized from the comparison of  $E_a$  values with the data of their optical band gap reported in [15]). The hopping conduction mechanism between localized states has been justified and presented in our previous works [15, 17].

To justify that the proposed electrothermal model (see Eq. 3) is suitable or not, we also have plotted theoretical (simulated) I–V curves of the samples (using the experimental values of  $E_a$ ,  $\alpha$ , and  $R_\infty$ ) in which Fig. 7 shows the typical such plot for TVSb5 sample. Another samples show similar behavior. As shown in Fig. 7, this theoretical

curves show the general treatment of NR in our experimental reports; in other word, this model is in good consistency with our experimental results. Also, as indicated in Fig. 7, the temperature in the bulk of samples increase during experiment and help to NR/switching to be occur.

Now, we can further discuss the non-ohmic region of I–V curves (a region before threshold voltage). One can define this region as pre-breakdown region in which thermal effects are not suitably detectable. As mentioned in “Electrical behaviour” section, this region (region of deviation from Ohm’s law) can be discussed to a bulk effect named as Pool–Frenkel effect. In this region, at a given temperature, dc electric field exerted on the sample can lower the potential barrier of carriers in the polaronic conduction (hopping conduction) mechanism and the current ( $I$ ) obtained as [4.5.10]

$$I \propto \exp\left(\frac{e \beta_{PF} E^{1/2}}{KT}\right) \tag{4}$$

and then

$$\ln(I) = const + \frac{e \beta_{PF} E^{1/2}}{KT}, \tag{5}$$

where  $\beta_{PF} = (e/\pi k)^{1/2}$ ,  $k = \epsilon \epsilon_0$ .  $\beta_{PF}$ ,  $\epsilon$ , and  $\epsilon_0$  are the potential barrier lowering factor, high-frequency dielectric constant, and vacuum dielectric constant, correspondingly. An almost linear relation between  $T \ln(I)$  and  $E^{1/2}$  is obtained when the electric field is about  $(10^3-10^4)V/cm$ . In other word, as temperature increases, the electric field required for the onset of non-ohmic behavior is reduced due to the increasing of electrical conduction originated from the semiconducting nature of the samples. Namely, the Pool–Frenkel effect is thermal excitation supported by an external high electric field. In brief, from Fig. 3 for

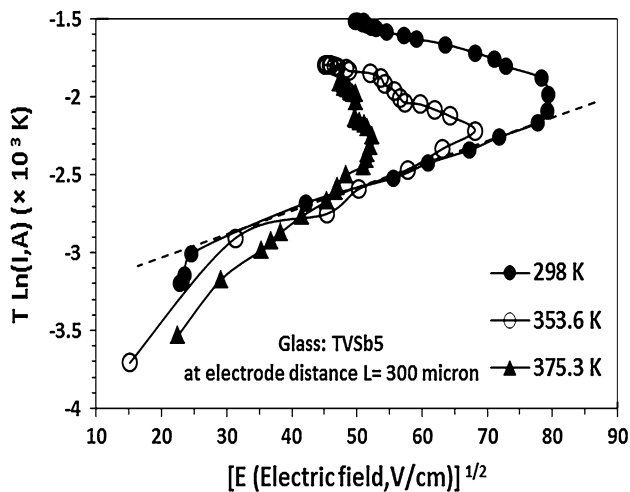


**Fig. 8** Pool-Frenkel plots for TVSb5 at different temperatures (dashed line shows schematically the linear part at 298 K, as a guide for eye)

TVSb5 and also for another samples, the lowering factor  $\beta_{PF}$  can be determined from the slope of the linear part of the  $T \ln(I)$  versus  $E^{1/2}$  plots. Pool-Frenkel plots are shown typically in Fig. 8 for TVSb5; all obtained values of  $\beta_{PF}$  are listed in Table 1. For each sample, the  $\beta_{PF}$  value increases with increase of temperature, which reveals the thermal effects besides the effect of electric field; therefore, this result justifies the electrothermal model.

## Conclusion

The NR/switching phenomena of ternary  $V_2O_5$ -Sb- $TeO_2$  glasses have been discussed on the basis of the electrothermal model. Crystallized current filaments, which may be formed between the electrodes in the bulk of samples, cause the electrical conductivity to increase. The glass composition and nature of the glassy matrix mainly control the threshold voltage. Increasing the Sb content of the glass increases the threshold voltage except for TVSb12 and 15. The tendency of crystallization (or in better word, decreasing of glass stability) of these glasses reduces the threshold voltage. The electrothermal model is the most applicable mechanism for the studied glasses.

## References

- Ovshinsky SR (1959) How liquid-state switch controls a-c. *Electronics* 32:76–81
- Marquez E, Villares P, Jimenezgaray R (1988) On non-ohmic conduction and the threshold characteristics of a bulk-type switching device based on the chalcogenide glassy semiconductor  $As_{0.40}Se_{0.30}Te_{0.30}$ . *J Non-Cryst Solids* 105:123–133
- Mirzai M, Hekmatshoar MH (2013) Study of electrical conductivity and memory switching in the zinc-vanadium-phosphate glasses. *Phys B* 420:70–73
- Mirzai M, Hekmatshoar MH (2013) Electrical switching in the CuO-ZnO- $P_2O_5$  glasses. *Phys B* 405:4505–4508
- Souri D, Elahi M, Yazdanpanah MS (2008) Pool-Frenkel Effect and High Frequency Dielectric Constant Determination of Semiconducting  $P_2O_5$ - $Li_2MoO_4$ - $Li_2O$  and  $P_2O_5$ - $Na_2MoO_4$ - $Na_2O$  Bulk Glasses. *Cent Eur J Phys* 6(2):306–310
- Montani RA, Robledo A, Bazan JC (1998) On the behavior of the I-V characteristic curves on  $TeO_2$ - $V_2O_5$ -based glasses. *Mater Chem Phys* 53(1):80–82
- Hirashima H, Watanabe Y, Yoshida T (1987) Switching of  $TiO_2$ - $V_2O_5$ - $P_2O_5$  glasses. *J Non-Cryst Solids* 95(96):825–832
- Mansour E, Mmustafa Y, El-Damrawi GM, Abd El-Maksoud S, Doweidar H (2001) Memory switching of  $Fe_2O_3$ -BaO- $V_2O_5$  glasses. *Phys B* 305:242–249
- Elahi M, Souri D (2002) Effect of High Electric Field on Conduction of  $TeO_2$ - $V_2O_5$ - $MoO_3$  Amorphous Thin Films. *Indian J Pure Appl Phys* 40:620–623
- Souri D, Elahi M (2006) Effect of High Electric Field on The DC Conduction of  $TeO_2$ - $V_2O_5$ - $MoO_3$  Amorphous Bulk Material; Czechoslovak. *J Phys* 56(4):419–425
- Lebrun N, Levy M, Souquet JL (1990) Electronic conductivity in glasses of the  $TeO_2$ - $V_2O_5$ - $MoO_3$  system. *Solid State Ionics* 40–41:718–722
- Pal M, Hirota K, Tsujigami Y, Sakata H (2001) Structural and electrical properties of  $MoO_3$ - $TeO_2$  glasses. *J Phys D Appl Phys* 34:459–464
- Jose R, Suzuki T, Ohishi Y (2006) Thermal and optical properties of  $TeO_2$ -BaO-SrO- $Nb_2O_5$  based glasses: New broadband Raman gain media. *J Non-Cryst Solids* 352:5564–5571
- Murugan GS, Suzuki T, Ohishi Y (2005) Tellurite glasses for ultrabroadband fiber Raman amplifiers. *Appl Phys Lett* 86(1):161109–1611012
- Souri D, Mohammadi M, Zaliani H (2014) Effect of antimony on the optical and some physical properties of Sb- $V_2O_5$ - $TeO_2$  glasses. *Electron Mater Lett* 10(6):1103–1108
- Sawa A (2008) Resistive switching in transition metal oxides. *Mater Today* 11:28–36
- Souri D, Azizpour P, Zaliani H (2014) Electrical conductivity of  $V_2O_5$ - $TeO_2$ -Sb glasses at low temperatures. *J Electron Mater* 43:3672–3680
- Abdel MM (2006) Aziz; Memory switching of germanium tellurium amorphous semiconductor. *J Appl Surf Sci* 253:2059–2065
- Fritzsche H (1974) Switching and memory in amorphous semiconductors. In: Tauc J (ed) *Amorphous and Liquid Semiconductors*. Plenum Press, London, pp 313–359
- Avila A, Asomoza R (2000) Switching in coplanar amorphous hydrogenated silicon devices. *Solid-State Electron* 40:17–27
- Abdel A (2000) All, A. Elshafie, M.M.Elhawary; DC electric-field effect in bulk and thin-film  $Ge_5As_38Te_57$  chalcogenide glass. *Vacuum* 4:845–853
- Wagle S, Shirodkar V (2000) Current controlled negative resistance phenomenon in SbPbSe system. *Czechoslov J Phys* 5:635–643
- Warren AC (1968) Switching mechanism in chalcogenide glasses. *Electron Lett* 5–12:461–462
- Henish HK, Fagen EA, Oshinsky SR, Fritzsche HF (1970) A qualitative theory of electrical switching processes in monostable amorphous structures. *J Non-Cryst Solids* 4:538–547